

INDUSTRIALLY RELEVANT Al₂O₃ DEPOSITION TECHNIQUES FOR THE SURFACE PASSIVATION OF Si SOLAR CELLS

Jan Schmidt,¹ Florian Werner,¹ Boris Veith,¹ Dimitri Zielke,¹ Robert Bock,¹ Veronica Tiba,²
Paul Poodt,³ Fred Roozeboom,^{3,4} Andrew Li,⁵ Andres Cuevas⁵ and Rolf Brendel¹

¹Institute for Solar Energy Research Hamelin (ISFH), Am Ohrberg 1, 31860 Emmerthal, Germany

²SoLayTec, PO Box 6235, 5600 HE Eindhoven, The Netherlands

³TNO Science & Industry, PO Box 6235, 5600 HE Eindhoven, The Netherlands

⁴Eindhoven University of Technology, Dept. of Applied Physics, PO Box 513, 5600 MB Eindhoven, The Netherlands

⁵School of Engineering, Australian National University (ANU), Canberra ACT 0200, Australia

ABSTRACT: We present independently confirmed efficiencies of 21.4% for PERC cells with plasma-assisted atomic-layer-deposited (plasma ALD) Al₂O₃ rear passivation and 20.7% for cells with thermal ALD-Al₂O₃. Additionally, we evaluate three different industrially relevant techniques for the deposition of surface-passivating Al₂O₃ layers on 1- Ω cm *p*-type silicon wafers, namely high-rate spatial ALD (*spatial ALD*), plasma-enhanced chemical vapour deposition (*PECVD*) and *reactive sputtering*. Using spatial ALD and PECVD, surface recombination velocities (SRVs) below 10 cm/s are obtained. Sputtered Al₂O₃ layers still provide an SRV of 35 – 70 cm/s. Despite their lower passivation quality compared to the Al₂O₃ films deposited by spatial ALD and by PECVD, we demonstrate that the sputtered Al₂O₃ layers are still suitable for the fabrication of 20.1% efficient PERC cells. After firing at ~800°C in a conveyor-belt furnace the SRV provided by the Al₂O₃ films deposited by spatial ALD is still below 20 cm/s, indicating an excellent firing stability. Both PECVD and sputtered Al₂O₃ passivation layers degrade to SRVs larger than 100 cm/s after firing. Hence, the firing stability of PECVD and – in particular – sputtered Al₂O₃ needs further optimisation.

Keywords: Silicon, Surface Passivation, Al₂O₃

1 INTRODUCTION

The use of thinner silicon wafers in the industrial silicon solar cell production combined with the aim of achieving higher efficiencies makes an effective control of surface recombination losses increasingly important. In recent years, aluminium oxide (Al₂O₃) films deposited by various techniques, such as atomic layer deposition (ALD), plasma-enhanced chemical vapour deposition (PECVD) and reactive sputtering, have proven capable of providing an effective surface passivation on low-resistivity *p*-type and *n*-type silicon wafers as well as on boron- and aluminium-doped *p*⁺-emitters [1-9]. In this contribution, we systematically compare the passivation quality of Al₂O₃ films deposited by various deposition techniques. Atomic layer deposition performed in lab reactors (plasma-assisted as well as thermal ALD) is limited to extremely low deposition rates (<2 nm/min), making such reactors unsuitable for industrial solar cell production. On the other hand, *high-rate spatial ALD*, *PECVD*, and *reactive sputtering* have an enormous potential for a transfer of Al₂O₃ into industrial cell production.

2 ATOMIC LAYER DEPOSITION

In the ALD process, one monolayer of Al₂O₃ is grown per cycle. Each cycle consists of two half-reactions, as depicted in Fig. 1. In the first half-reaction, trimethyl aluminium (TMA) molecules react with hydroxyl (OH) groups attached to the surface. At the end of the first half-reaction, Al atoms and methyl groups cover the surface and the remaining TMA molecules in the deposition chamber are no longer able to react with the surface. After purging the deposition chamber with inert or oxygen gas, the second half-reaction of the ALD cycle starts. We apply two different realization forms for the second half-reaction: in the *thermal ALD* process, water vapor is injected into the deposition chamber. The H₂O molecules react very fast with the Al-CH₃ complex at-

tached to the surface. Hydrogen reacts with the methyl group to form methane, and oxygen reacts with aluminium to form aluminium oxide. In the plasma-assisted ALD (*'plasma ALD'*) process, an oxygen plasma is ignited above the substrate, generating oxygen radicals which effectively react with the methyl groups and the aluminium at the surface. In the FlexAL deposition system from Oxford Instruments applied in this study a remote inductively coupled plasma (ICP) source is used, which means that the oxygen plasma is not in direct contact with the silicon wafer during Al₂O₃ deposition. This type of remote-plasma deposition technique is known to create almost no plasma damage at the surface, and is hence well suited for an excellent silicon surface passivation.

In a conventional ALD process, the separation of the half-reactions is implemented by alternate dosing of the process gases. Exposure times of only a few milliseconds are sufficient to ensure complete saturation of the growth surface. In between both precursor doses, however, the reactor chamber is purged by an inert gas and subsequently pumped to remove the residual process gas and reaction products. To prevent parasitic CVD processes and ensure a true ALD process, pumping times of the order of a few seconds are required, severely limiting the growth rate to approximately 2 nm/min. This makes conventional ALD unsuitable for high-throughput industrial solar cell production.

Recently, Poodt et al. proposed a high-rate fast ALD concept based on spatially separated ALD (*'spatial ALD'*) [10], enabling deposition rates of 70 nm/min. In contrast to the conventional sequential separation, both half-reactions are *spatially* separated (see Fig. 2), thus eliminating the need for intermediate pumping steps. In a first proof-of-principle lab tool developed at TNO [10], the spatial separation was achieved by rotating the wafer underneath a round reactor head incorporating gas inlets for TMA and water vapor, separated by gas bearing planes formed by a flow of pressurized nitrogen. Since both reaction zones are sealed off by nitrogen flow, any

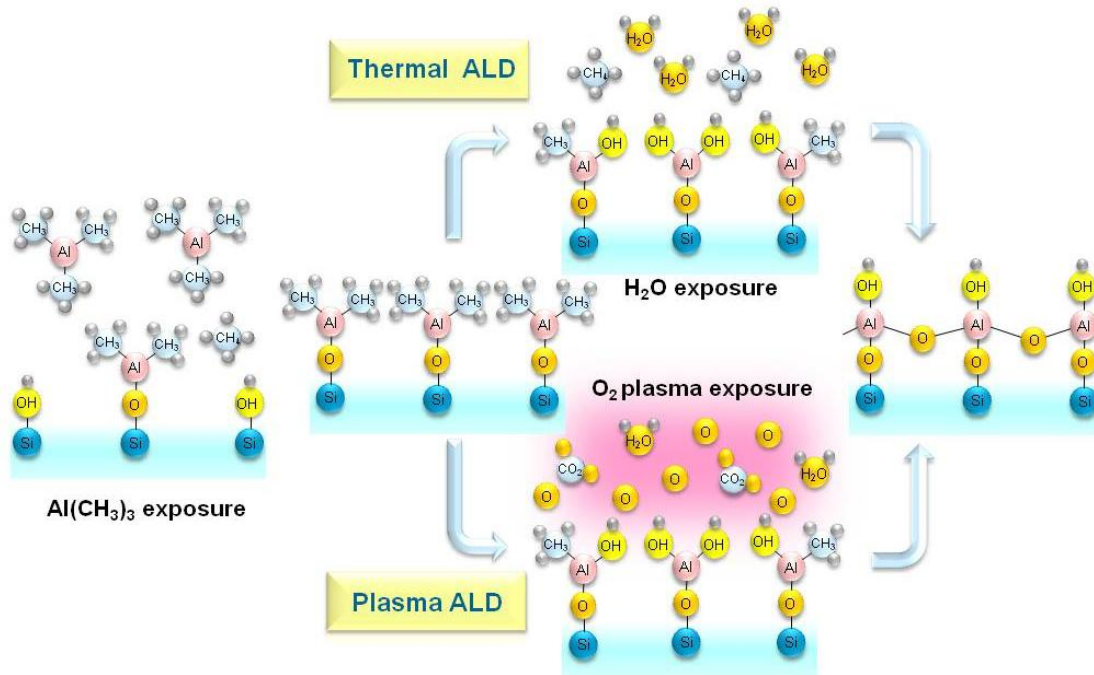


Fig.1. Schematic of one cycle of a thermal and a plasma-assisted atomic layer deposition (ALD) process. Each cycle consists of two half-steps: first, the trimethyl aluminium (TMA) molecules attach to the hydroxyl groups attached to the silicon surface; second, the molecules are oxidized by H₂O (thermal ALD) or an O₂ plasma (plasma ALD).

unintentional interaction of the process gases is prevented and the deposition can be performed under atmospheric conditions, an additional advantage concerning the industrial applicability.

Figure 3 shows the effective lifetimes τ_{eff} measured as a function of the injection density Δn for 1.3 Ωcm *p*-type float-zone silicon (FZ-Si) wafers passivated using Al₂O₃ deposited by plasma-assisted, thermal and spatial ALD. Lifetimes were measured by the photoconductance decay (PCD) method using a Sinton lifetime tester. All Al₂O₃ films received a post-deposition anneal at (400±50)°C for ~15 min to activate the surface passivation [11]. As can be seen from Fig. 3, all 3 ALD techniques result in Al₂O₃ films of outstanding surface passivation quality, which shows an extremely weak injection dependence over the complete relevant injection range between 10¹³ and 10¹⁵ cm⁻³. Al₂O₃ deposited by plasma ALD provides effective lifetimes between 3 and 4.8 ms in the relevant injection range. The measured lifetime of 4.8 ms at $\Delta n = 10^{15}$ cm⁻³ lies well above the commonly used empirical expression for the intrinsic lifetime limit for crystalline silicon [12], indicating a nearly perfect surface passivation. It is clear that the expression for the intrinsic lifetime limit needs to be updated. Assuming an infinite bulk lifetime, we can calculate an upper limit to the surface recombination velocity (SRV) S_{max} using the simple relation $S_{\text{max}} = W/2\tau_{\text{eff}}$, where $W = 290 \mu\text{m}$ is the wafer thickness. Using this relation, $\tau_{\text{eff}} = 4.8$ ms corresponds to an upper SRV limit of $S_{\text{max}} = 3$ cm/s.

Most importantly, it can be deduced from Fig. 3 that both traditional thermal ALD as well as spatial ALD provide Al₂O₃ films with an extremely high level of surface passivation, as indicated by lifetimes of 2 ms, corresponding to an upper SRV limit of $S_{\text{max}} = 7$ cm/s, for both techniques and a practically negligible injection dependence over the relevant injection range. It is quite remar-

able that the high-rate (in our case 14 nm/min) spatial ALD produces exactly the same excellent level of surface passivation as the slow (< 2 nm/min) thermal ALD.

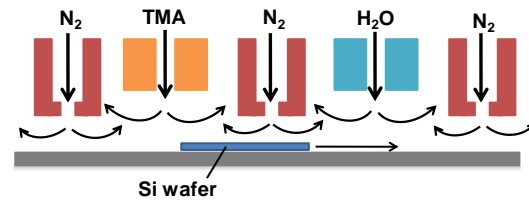


Fig. 2. Schematic of the 'spatial ALD' concept [10]. The TMA and water half-reaction zones are separated by N₂ gas bearings.

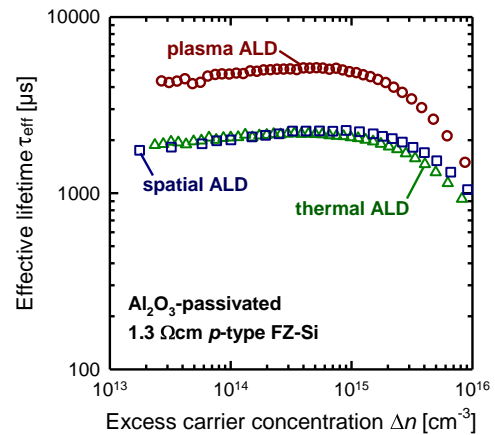


Fig. 3. Effective lifetime τ_{eff} as a function of the injection density Δn measured on 1.3 Ωcm *p*-type FZ-Si passivated by Al₂O₃ deposited by plasma, thermal and spatial ALD.

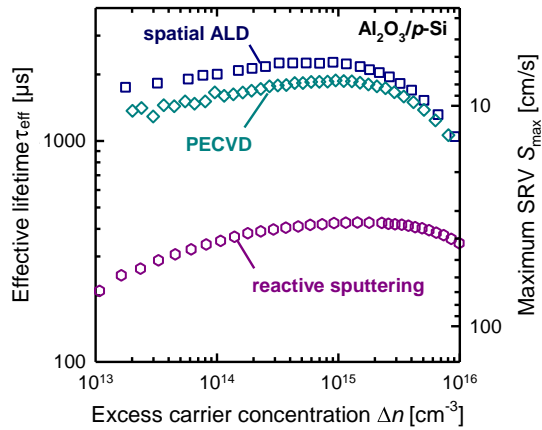


Fig. 4. Effective lifetime τ_{eff} (left scale) and upper surface recombination velocity (SRV) limit S_{max} (right scale) as a function of the injection density Δn measured on 1.3 Ωcm p -type FZ-Si passivated by Al_2O_3 deposited by spatial ALD, PECVD, and reactive sputtering.

3 Al_2O_3 DEPOSITION TECHNIQUES SUITABLE FOR INDUSTRIAL CELL PRODUCTION

Recently, two other techniques were demonstrated to be suitable for depositing surface-passivating Al_2O_3 layers. Plasma-enhanced chemical vapour deposition (PECVD) [5,7] was shown to provide SRVs of only 10 cm/s on 1- Ωcm p -type FZ-Si, whereas reactive sputtering [8] on comparable material resulted in SRVs down to 55 cm/s. In this paper, we have studied the passivation quality of Al_2O_3 deposited by microwave-remote PECVD (Roth&Rau SiNA) and by rf magnetron sputtering (homemade setup at ANU). The sputtering uses an aluminium target, which is reactively sputtered in an O_2/Ar atmosphere [8], while the PECVD uses TMA and nitrous oxide as process gases.

Figure 4 compares the effective lifetimes we have measured on 1.3 Ωcm p -type FZ-Si wafers passivated by Al_2O_3 films deposited using the, in our opinion, most promising industrial Al_2O_3 deposition techniques: (i) spatial ALD, (ii) PECVD, and (iii) rf magnetron sputtering. The direct lifetime comparison in Fig. 4 shows that both spatial ALD and PECVD provide S_{max} values < 10 cm/s, clearly outperforming the sputtered Al_2O_3 . Nevertheless, the sputtered Al_2O_3 passivation layer results in an S_{max} between 35 and 70 cm/s in the relevant injection range, which would be still sufficient for the next generation of industrial high-efficiency solar cells.

A very important property is the stability of the surface passivation during a firing step as it is typically applied in the screen-printing metalisation of solar cell production lines. We have hence annealed the samples of Fig. 4 in an industrial infrared conveyor-belt furnace (Centrotherm Contact Firing Furnace DO 8.600-300-FF) at a peak temperature of $\sim 800^\circ\text{C}$. Figure 5 shows the SRVs measured before and after firing. The Al_2O_3 deposited by spatial ALD shows clearly the best firing stability, providing SRVs below 20 cm/s at $\Delta n = 10^{15} \text{ cm}^{-3}$ after firing, whereas the Al_2O_3 layers deposited by PECVD result in $S_{\text{max}} = 125$ cm/s and that of the sputtered Al_2O_3 results in $S_{\text{max}} = 390$ cm/s. Obviously, the PECVD- Al_2O_3 and – in particular – the sputtered Al_2O_3 need further op-

timisation. One possibility to improve the firing stability could be to use double layers of Al_2O_3 , deposited by PECVD or sputtering, and a PECVD- SiN_x or PECVD- SiO_x on top. $\text{Al}_2\text{O}_3/\text{SiN}_x$ stacks have already proven to result in an improved firing stability for ultrathin ALD- Al_2O_3 layers [9].

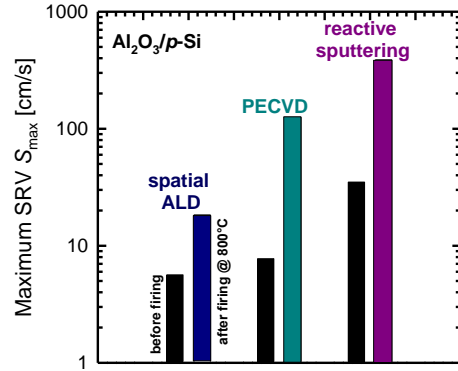


Fig. 5. Surface recombination velocity (SRV) S_{max} measured at an injection level of $\Delta n = 10^{15} \text{ cm}^{-3}$ for 1.3 Ωcm p -type FZ-Si passivated by Al_2O_3 deposited by spatial ALD, PECVD, and reactive sputtering before and after firing at $\sim 800^\circ\text{C}$.

4 PERC SOLAR CELLS

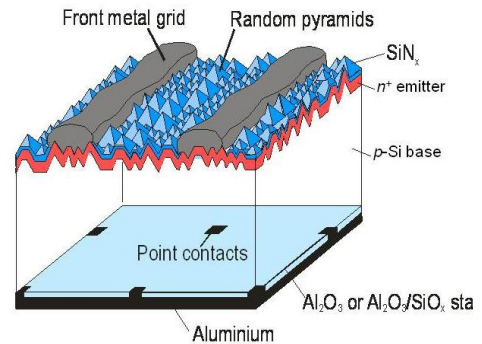


Fig. 6. PERC-type solar cell structure used to demonstrate the applicability of different rear surface passivation schemes.

We have implemented Al_2O_3 rear passivation layers deposited by plasma ALD, thermal ALD and sputtering into passivated emitter and rear cells (PERC) using the process sequence described in Ref. 3. Figure 6 shows the cell structure featuring a PECVD- SiN_x -passivated 100 Ω/sq phosphorus-diffused n^+ front emitter and a rear surface passivated by the dielectric layer systems shown in the first column of Table 1. The front grid is made by shadow-mask evaporation of aluminium and the rear is fully metalised by aluminium evaporation (4% rear metal contact fraction) after point contact openings have been generated. As a reference process we use a SiO_2 rear passivation grown by wet thermal oxidation at 1000°C [3]. Table 1 summarizes the one-sun parameters of the best PERC solar cells, as measured under standard testing conditions (25°C , $100 \text{ mW}/\text{cm}^2$, AM 1.5 G). The measured open-circuit voltages V_{oc} and short-circuit current densities J_{sc} of the ALD-passivated cells are higher than the V_{oc} and J_{sc} values of the sputtered cell and the SiO_2 -passivated reference cell.

Table 1: One-sun parameters measured under standard testing conditions of the best PERC silicon solar cells with 4 different rear surface passivations: (i) thermal SiO₂ (220 nm), (ii) thermal ALD Al₂O₃ (30 nm)/PECVD-SiN_x (100 nm) stacks, (iii) plasma ALD Al₂O₃(30 nm)/PECVD-SiO_x (200 nm) stacks, and (iv) sputtered Al₂O₃ (110 nm). All cells were fabricated on 0.5-Ωcm FZ *p*-Si wafers. The aperture cell area is 4 cm².

Rear side passivation	V _{oc} [mV]	J _{sc} [mA/cm ²]	FF [%]	η [%]
Thermal SiO ₂	657	39.1	78.9	20.2
Thermal ALD Al ₂ O ₃ /SiN _x	662	40.6	76.9	20.7*
Plasma ALD Al ₂ O ₃ /SiO _x	664	40.7	79.4	21.4*
Sputtered Al ₂ O ₃	651	39.1	79.1	20.1*

*independently confirmed at ISE Callab

V_{oc} values of ALD-passivated cells are all >660 mV and J_{sc} values are >40 mA/cm², demonstrating the huge potential of ALD for the rear surface passivation of PERC-type cells. On top of the very thin ALD-Al₂O₃ layers we have deposited thicker PECVD-SiO_x or SiN_x layers to improve the internal rear reflection of the cell. The independently confirmed record-high conversion efficiencies are **21.4%** for the **plasma ALD-Al₂O₃** rear passivation and **20.7%** for the **thermal ALD-Al₂O₃** passivation. The passivation quality of the sputtered Al₂O₃ is clearly inferior to that of the ALD-Al₂O₃ films, as indicated by an ~10 mV lower V_{oc} and an ~1.5 mA/cm² reduced J_{sc}. Still our PERC cells with **sputtered Al₂O₃** as rear passivation achieve an independently confirmed efficiency of **20.1%**.

5 CONCLUSIONS

Using spatial ALD and PECVD, SRVs below 10 cm/s were measured on 1.3-Ωcm *p*-type silicon. Sputtered Al₂O₃ layers provided SRVs in the range of 35 – 70 cm/s on the same material. Despite their lower passivation quality compared to the Al₂O₃ films deposited by spatial ALD and by PECVD, we have demonstrated that the sputtered Al₂O₃ layers are still suitable for the fabrication of PERC cells with an efficiency of 20%. After firing at ~800°C in a conveyor-belt furnace, the SRV provided by the Al₂O₃ films deposited by spatial ALD was found to be below 20 cm/s, indicating an excellent firing stability of the layers deposited by spatial ALD. On the other hand, both PECVD and sputtered Al₂O₃ passivation layers degraded to SRVs larger than 100 cm/s after firing. We conclude that spatial ALD is already well compatible with screen-printing, while the firing stability of PECVD and sputtered Al₂O₃ needs further optimisation.

ACKNOWLEDGEMENTS

Funding was provided by the State of Lower Saxony and the German Ministry for the Environment, Nature Conservation and Nuclear Safety (BMU) under contract number 0325050 (“ALD”).

REFERENCES

- [1] G. Agostinelli, A. Delabie, P. Vitanov, Z. Alexieva, H.F.W. Dekkers, S. De Wolf, G. Beaucarne, *Sol. En. Mat. Sol. Cells* **90**, 3438 (2006).
- [2] B. Hoex, J. Schmidt, P. Pohl, M. C. M. van de Sanden, W. M. M. Kessels, *J. Appl. Phys.* **104**, 044903 (2008).
- [3] J. Schmidt, A. Merkle, R. Brendel, B. Hoex, M.C.M. van de Sanden, W.M.M. Kessels, *Progr. Photovolt.* **16**, 461 (2008).
- [4] J. Benick, B. Hoex, M. C. M. van des Sanden, W. M. M. Kessels, S. W. Glunz, *Appl. Phys. Lett.* **92**, 253504 (2008).
- [5] I. Cesar, E. Granneman, P. Vermont, E. Tois, P. Manshanden, L. J. Geerligs, E. E. Bende, A. R. Burgers, A. A. Mewe, Y. Komatsu, and A. W. Weeber, *Proc. 35th IEEE PVSC*, Honolulu, HI (2010), in press.
- [6] S. Miyajima, J. Irikawa, A. Yamada, and M. Kona-gai, *Proc. 23rd EUPVSEC*, Valencia, Spain (2008), p. 1029.
- [7] P. Saint-Cast, D. Kania, M. Hofmann, J. Benick, J. Rentsch, R. Preu, *Appl. Phys. Lett.* **95**, 151502 (2009).
- [8] T. T. Li and A. Cuevas, *Physica Status Solidi – Rapid Research Letters* **3**, 160 (2009).
- [9] J. Schmidt, B. Veith, R. Brendel, *Physica Status Solidi – Rapid Research Letters* **3**, 287 (2009).
- [10] P. Poodt, A. Lankhorst, F. Roozeboom, K. Spee, D. Maas, and A. Vermeer, *Advanced Materials* **22**, 3564 (2010).
- [11] J. Schmidt, B. Veith, F. Werner, D. Zielke, and R. Brendel, *Proc. 35th IEEE PVSC*, Honolulu, HI (2010), in press.
- [12] M. J. Kerr and A. Cuevas, *J. Appl. Phys.* **91**, 2473 (2002).